Ecological Indicators 148 (2023) 110116

Contents lists available at ScienceDirect

Ecological Indicators

journal homepage: www.elsevier.com/locate/ecolind

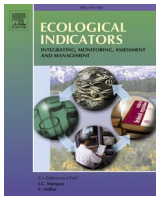

TLidar-based crown shape indicates tree ring pattern in Norway spruce (*Picea abies* (L.) H. Karst) trees across competition gradients. A modeling and methodological approach

Shamim Ahmed *, Hans Pretzsch

Chair of Forest Growth and Yield Science, Department of Life Science Systems, TUM School of Life Sciences, Technical University of Munich, Hans-Carl-von-Carlowitz-Platz 2, 85354 Freising, Germany

ARTICLE INFO

Keywords:
Regular and irregular growth patterns
Crown architecture
Beta-distributions
Competition reduction
Transgressive growth
Machine learning
Terrestrial laser scanning (TLS)

ABSTRACT

Tree crowns and growth rings are physiologically and functionally connected through supporting and resource sharing. Management interventions may strongly influence tree growth by altering this linkage. However, conventional approaches have limited ability to characterize crown shape precisely, thus hindering our understanding of the relationship between crown shape and tree ring patterns. We, thus, aimed to test three hypotheses: (HI) Crown shape (regularity vs. irregularity) and ring patterns (regularity or irregularity) are significantly correlated and (HII) vary across density gradients; if so, (HIII) internal ring patterns could be predicted from external crown shape metrics. We, therefore, employed terrestrial laser scan-based crown shape and coring-based TRP metrics for Norway spruce (*Picea abies* (L.) H. Karst.) trees covering a range of density gradients to assess temporal changes of crown shape and tree ring patterns. We found a significant and positive influence of crown shape quantifying metrics on ring patterns, indicating crown regularity or irregularity strongly reflects tree ring regularity or irregularity ($p < 0.05$). Crown shape and ring patterns always showed comparable patterns across density gradients (e.g., trees from lower-density stands produced transgressive crown and ring growth) and significantly varied across competition level. Trees grown in lower-density stands are more likely to produce upper-reaching crowns (maximum crown radius expansion shifted to the mid- to upper-crown) than trees grown in competitive conditions, which result in lower-reaching crowns (maximum crown radius shifted to the crown base) with reduced crown shape and ring pattern parameters. Crown irregularities increased as density decreased through competition reduction, resulting in more regular ring patterns (stable growth). Since both crown shape and ring patterns are simultaneously impacted by stand density or competition, the relationship between crown shape and ring patterns is competition-neutral. When viewed separately, both patterns had a strong relationship with the competition index. Finally, our comparative model predictions showed that approaches ranging from simple linear models to complex machine learning techniques (e.g., random forest, neural network, support vector machine, etc.) were effective in predicting ring patterns using external TLidar-crown shape, indicating a potential method to evaluate the crown shape and ring pattern link. The relationship between the crown and growth ring and their synchronous patterns across competition gradients suggests that internal growth can be assessed from the external appearances of trees and recommends further consideration in forest modeling.

1. Introduction

A tree's crown and annual ring are functionally linked through resource sharing. For example, a tree leaf is responsible for photosynthesis, which critically determines the stem increment, while the stem provides hydraulics and mechanical supplies to the leaves (Esser, 1946; Lehnebach et al., 2018). More specifically, stem vessel elements conduct water and nutrients through the branches to the leaves (Grote and Pretzsch, 2002; West et al., 2009) to continue photosynthetic work while the crown translocates carbon to the stem (Hemery et al., 2005; Kalliovirta and Tokola, 2005; Kramer, 2012). Besides, to support bigger leaves, a bigger stem is required (Corner, 1949), which creates a

* Corresponding author.
E-mail address: shamim.ahmed@tum.de (S. Ahmed).

https://doi.org/10.1016/j.ecolind.2023.110116
Received 2 January 2023; Received in revised form 2 March 2023; Accepted 6 March 2023

functional linear bridge between the crown and the tree ring. Similarly, pipe model theory explains that crown foliage leaves and stem tissue or sapwood dimensions are linearly correlated (Lehnebach et al., 2018; Shinozaki et al., 1964). This relationship can also be traced back to Pressler's Law (Pressler, 1865). In addition, the main predictions of metabolic scaling theory (MST) are the photosynthesis rate and metabolic rate, which are scaled up with biomass growth and can be scaled up with stem diameter growth (Enquist et al., 2007; Enquist et al., 1999; Shenkin et al., 2020). Therefore, it is important to uncover possible quantitative relationships along with functional relationships between the crown architecture and tree rings. (Julio Camarero et al., 2018; Mäkelä and Valentine, 2006; Pretzsch et al., 2022). Nonetheless, a better understanding of the internal and external structure relationships could also improve the MST predictions (Pretzsch, 2021b; Shenkin et al., 2020; West et al., 2009).

Besides, crown-related functional and morphological traits (i.e., crown profiles, branch, and leaf traits) are critical in determining the evolutionary and phylogenetic relationships of species (Antonarakis et al., 2010; Arslan et al., 2021; Kokaly et al., 2009; Wright et al., 2006), evaluating the environment or climatic stressors (e.g., drought) (Chaturvedi et al., 2011; Jacobs et al., 2021; Junttila et al., 2021); and understanding the stand and carbon dynamics (Rawat et al., 2015). Thus, evaluating crown and tree ring properties is crucial in forest ecology not only for understanding prior historical and legacy effects such as drought but also management impacts (Jacobs et al., 2021; Lüttge and Hertel, 2009; Netzer et al., 2019; Ogle et al., 2015; Pearl et al., 2020; Pretzsch, 2021a, b; Shenkin et al., 2020), because management and its prior history or ecological legacy mostly reflect on crown and tree ring patterns (Lüttge and Hertel, 2009). Furthermore, a tree's crown and annual ring retain similar information, and therefore both are widely employed in many growth modeling techniques. For example, many eco-physiological models used a combination of internal (such as sapwood area) and external (such as leaf area, crown width, etc.) tree characteristics to predict growth (Grote and Pretzsch, 2002; Pretzsch, 2021b; Sievänen et al., 2000). Tree growth models can be improved by including crown (e.g., projection area, ratio, etc.) and tree ring statistical variables (e.g., ring width and standard deviation of ring width) (Pretzsch, 2021b). As a result, quantifying crown structure and tree ring pattern relationships would have a significant impact on tree growth modeling.

Although there have been a few attempts to quantify the relationships between crown size or condition and tree ring or diameter growth (Anderson-Teixeira et al., 2015; Drobyshev et al., 2007; Pretzsch, 2019; Pretzsch et al., 2022; Pretzsch and Rais, 2016; Shenkin et al., 2020; Sundberg et al., 1993; Tallieu et al., 2020), the relationships between crown shape and tree ring patterns explaining metrics have rarely been studied. This gap comes from the limitations of crown shape characterization with traditional methods, but this gap is being filled with the advent of terrestrial laser scanning (TLS) technology (Barbeito et al., 2017; Bayer et al., 2013). TLS data provides ample scope to depict crown shape from several axes and more precisely (Calders et al., 2020; Metz et al., 2013; Olivier et al., 2016), which overcomes the methodological limitations of linking crown shape and tree ring patterns. For example, Rais et al. (2021) used TLS data to show a correlation between stem wood structure and crown structure. Besides, Shenkin et al. (2020) and Pretzsch et al. (2022) quantified the linkage between crown structure, stem diameter, and tree ring growth.

In addition, several studies observed crown shape variations across stand types (Barbeito et al., 2017), management interventions such as thinning (Köcher et al., 2012; Yen, 2015), site gradient, climate, species divergence (Poorter et al., 2006; Rawat et al., 2015), space available for expansion, exposed shoots, and cones produced (Schneider et al., 2020). Most specifically, in even-aged stands, interspecific competitions for resources (e.g., light, water, nutrients, etc.) may increase with increasing tree size (Kholdaenko et al., 2022; Xue et al., 2010). High-density growing conditions reduced tree diameter and crown (del Río et al., 2019; Kholdaenko et al., 2022). In turn, stem density reductions may benefit trees by making resources available for the remaining trees (Purahong et al., 2014). Crown shape can also change due to stand structural diversity, growth dominance, and competition intensity. For example, shade-tolerant and light-demanding trees produce very shallow, flat crowns and extended crowns with a monolayer or multilayer leaf pattern to maximize and decrease light interception (see Givnish (1988), Poorter et al. (2012)). When trees reach the canopy top, they prefer to develop a shallow but wide crown (Antin et al., 2013; Muller-Landau et al., 2006). Besides, numerous studies have linked stem growth and crown structure with forest management (Chhin et al., 2010; Montoro Girona et al., 2017; Yen, 2015), whereas crown shape and its relationships to management interventions are less known.

Growth prediction can improve the understanding of ecophysiological and statistical modeling (Mäkelä and Valentine, 2006). Overall, this understanding may help to manage forests sustainably in an improved way (Pretzsch et al., 2022). Prior and conventional growth prediction approaches were based on tree age and total mass (discussed in Pretzsch (2021b)), while growth prediction from the crown shape metrics is rarely focused due to methodological limitations. However, the link between crown shape (regularity or irregularity) and the regularity or irregularity of tree ring patterns with density gradients and reduction is poorly understood, which restricts our growth predictions.

We, thus, aimed to test three hypotheses: (HI) Tree ring statistical metrics and patterns (TRP) (regular vs. irregular) and crown shape (CS) patterns (regular vs. irregular) are significantly correlated, while (HII) CS and TRP variables strongly vary across density gradients or competition levels, depicting trees in high-competition stands producing a narrower and more irregular crown and tree ring than trees in lower density or competitive stands (Fig. 1). We also envisaged that (HIII) a set of external CS metrics could be used to predict internal TRP.

To test the hypotheses, multiple tree ring pattern metrics covering a range of stand density were utilized, along with several crown shape metrics.

2. Methods

2.1. Study site description

We scanned and cored 30 N. spruce from long-term, pure, even-aged experimental plots in Fürstenfeldbruck 612 (FFB612) in November 2021 (see Supplementary Fig. 1a for plot design), which were done by IUFRO with four-year-old seedlings in 1974 in southern Germany (longitude: 11.05° E and latitude: 48.14°N). The mean annual precipitation and temperature over the last 30 years (1991–2020) were 932 mm and 8.8 °C, respectively. The experimental sites consist of 21 plots (each of 900 m^2), covering ten different thinning-spacing combinations (see more about plots and study site descriptions in Schmied et al. (2022)). However, we collected our sample trees from four thinning-spacing combination plots to cover different competition levels (see Supplementary Fig. 1a), combining thinned and unthinned stands. Unthinned stands that we used as a reference stand after plantation were never thinned (due to high competition). To demonstrate the heterogeneity of impacts of density-based management on crown and tree ring patterns, trees from thinned stands were isolated based on different thinning intensities (high and low initial spacing vs. high and low thinning intensity) (Supplementary Fig. 1a).

2.2. Terrestrial laser scanning data acquisition and crown shape characterization

Terrestrial laser scanning (TLS) eases access to crown metrics (Pretzsch, 2021b) and is thus recognized as an effective tool for assessing crown size (Srinivasan et al., 2015). We scanned FFB612 with the RIEGL VZ-400i (RIEGL 2019) TLS. The scanned raw point clouds were automatically registered and filtered using an octree approach to enable

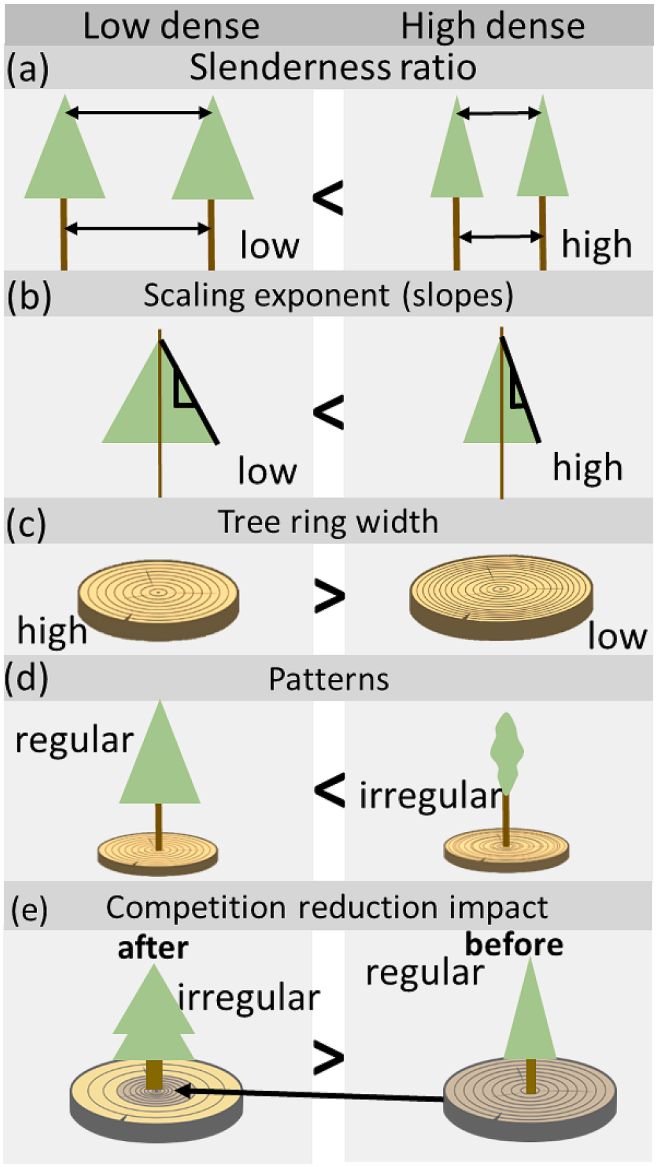

Fig. 1. Conceptualized coniferous tree crown developments explain tree ring patterns by folding into polar coordinates, where the Gaussian tree crown growth curve transforms into several tree ring patterns across low-density or thinned and high-density or unthinned stands. (a) Impact of density or competition on crown shape and tree ring patterns (increasing density increases slenderness (cl/cr) coefficient value but decreases plumpness coefficient (cr/cl) and growth) [crown radius (cr) and crown length (cl)]. (b) Crown scaling exponent (slopes of sun exposed crown) components; (c) Ring width variations; (d) regular crown shape and tree ring patterns and irregular crown shape and tree ring patterns in low and high dense stands. A high coefficient of variation (cv) of crown radius (cr) and tree rings (trw) denotes higher irregularity, while a low cv value denotes lower irregularity, indicating more regular crown and tree ring patterns. (e) Competition reduction promotes crown and tree ring growth while creating more irregular patterns due to previous low and current high growth combinations.

post-processing performance with RiSCAN PRO software (version 2.10.1). To prevent overlapping errors that could happen during automatic tree isolation, each tree was first identified using a coordinate system before being manually isolated from the stands. Individual tree point cloud data processing was done in R (version 4.2.1) (R Core Team 2022) by using "lidR" (Roussel et al., 2020), "dbscan" (Hahsler et al., 2019), and the "VoxR" package (Lecigne et al., 2018). Details of the scanning procedure, data processing, and R packages used for analysis can be found in Jacobs et al. (2022) and Pretzsch et al. (2022).

To understand crown shape and tree ring pattern relationships, we evaluated several crown and tree ring metrics (Table 1), as Pretzsch et al. (2022) explained that these relationships can be done with a few allometric relationships between crown and tree ring variables. Additionally, several studies have already identified and observed that the listed variables are somehow correlated to stem, diameter, and diameter growth (Franceschi et al., 2022; Pretzsch, 2021a, b, 2022; Pretzsch et al., 2022). Therefore, we used multiple crown shape (CS) and tree ring

Table 1
List of crown metrics and tree ring growth and pattern metrics used in this study. More details and visualizations can be found in Supplementary Fig. 2.

Sl. No.	Variables and metrics names	Abbreviated form	Explanation or calculation
Crown metrics			
1	Tree height	**h**	total tree size (vertical)
2	Crown base height (m)	**cbh**	lowest crown position (first living branch position)
3	Crown length or depth (m)	**cl**	difference between total tree height and crown base height (cl = h-cbh)
4	Crown width (cw)	**cw**	average crown expansion from the crown center
5	Crown ratio or percentage (%)	**cratio**	ratio between cl and h
6	Crown radius (m)	**cr**	$cr^{-} = \sqrt{((r_1^2 + r_2^2 + \ldots + r_8^2)/8)}$
7	Crown base radius	**cbr**	radius at the crown base point
8	Maximum cr	**maxcr**	maximum vertical crown distance from a specific crown height or the largest cr
9	Cumulative maxcr	**cumaxcr**	a greater vertical expansion from the x-axis (crown length) indicates a more even and consistent distribution of maxcr or crown volume along crown length.
10	Height of maxcr	**hmaxcr**	length from base to maxcr
11	Crown projection area (m^2)	**cpa**	crown's perpendicular projected area on the ground
12	Crown volume (m^3)	**cv**	volume of alpha hull (point clouds)
13	Top heaviness	**th**	the ratio between maxcr to the distance between maxcr and tree's tip
14	Slope of crown profiles	**scp**	slope or steepness estimate of crown distribution fitted by a linear model (y = mx + c, m = slopes)
15	Crown plumpness (or slenderness)	**cplc (cslc)**	ratio between crown radius (cr) and crown length (cl) (cl/cr)
16	Coefficient of variation of cr	**cvcr**	standard deviation (sd) of cr to mean cr ratio
17	Shape of beta distribution of crown	**ca, cb**	shape parameters for the cumulative (maxcr) crown. ca, cb correspond to crown width and crown length, respectively
Tree ring metrics			
1	stem current diameter	**d**	tree's current size (horizontal) or diameter at breast height
2	stem diameter increment or growth	**id**	sum of ring width in the N and E cardinal directions
4	Mean tree ring width (trw) (mm)	**trw**	total ring width/measured number of rings
5	Cumulative trw	**cutrw**	total trw increment
6	Coefficient of variation of trw	**cvtrw**	inter-annual variation of trw (cvtrw = sdtrw/mean trw)
7	Stability in trw	**strw**	inverse cvtrw (1/cvtrw)
8	trw skewness	**skewness**	a higher value indicates highly skewed or asymmetric tree ring (tree ring normality)
9	Shape of beta distribution of tree ring	**ta, tb**	shape parameters for the cumulative tree ring. ta, tb correspond to tree ring width and tree age or growth years, respectively

patterns (TRP) statistical metrics to correlate CS and TRP metrics.

2.3. Increment coring to characterize tree ring patterns

The same 30 trees were cored from the north and south cardinal directions (to avoid reaction wood) at diameter at breast height (130 cm) points using an increment borer (5 mm in diameter) (Haglöf, Sweden) for tree ring analysis (Pretzsch et al., 2013; Schweingruber, 2012). All of the cores (60 cores) were air dried, glued onto hardwood plates, and gradually sanded. Using a Lintab Series 5 and Tsap-Win software, tree ring width (TRW) was measured (Rinntech Heidelberg, Germany). Each core was visually cross-dated (details can be found in Schmied et al. (2022)), and additional analyses were performed using the "dplR" package in R (Bunn, 2008).

2.4. Statistical analyses

To demonstrate detailed statistical relations between crown shape and tree ring patterns and their variation across density gradients (HI), we used a three-step procedure. First, we fitted a two-parameter beta (β) distribution (Eqn. (1) to the crown profile and cumulative tree ring patterns.

$$f(x,a,b) = b_0 x^{a-1}(1-x)^{b-1} \quad (1)$$

where b_0 represents the normalization constant and a and b are shape variables (a > 0, b > 0). Besides, ca, cb, and ta, tb denote the crown and tree ring beta shape parameters, respectively (also see Table 1).

Later, we extracted shape parameters and used them in bivariate relationships to examine the relationships between crown and tree ring β-shape parameters. Bivariate relationships helped us analyze the link between crown shape regularity or irregularity and tree ring pattern metrics (e.g., regularity or irregularity). We also fitted a linear regression (y = mx + c) model to each tree's crown profile (sun exposed crown) and retrieved its slopes (m) to determine whether the distribution (steepness) of the tree's crown profile influences the patterns of tree ring width or asymmetry (skewness).

Second, to determine the variability of the shape parameters for the crown (ca and cb, representing crown width and length) and tree rings (ta and tb, representing to ring width and age) across density gradients or competition gradients (HII), we compared the patterns β-distributions relevant to the shape variables. This was accomplished through the use of a one-way analysis of variance (ANOVA).

Third, we fitted a linear mixed model (Eqn. 2) to investigate the effect of stand density or competition, stand types (thinned or unthinned), and individual tree level on crown shape and tree ring pattern relationships using the "lme4″ and "lmerTest" packages in R (Bates, 2010; Kuznetsova et al., 2017).

$$\mathrm{TRP_{ij}} = \mathrm{a_o} + \mathrm{a_1\ CSV_{ij}} + \mathrm{a_2\ year_{ij}} + \mathrm{a_3\ SDI_i} + \mathrm{a_4\ CSV_{ij} \times year_i} + \mathrm{b_i} + \varepsilon_{ij} \quad (2)$$

where TRP, CSV, and SDI denote tree ring pattern variables, TLS-derived crown shape variables, and mean stand density index SDI, respectively.

$$SDI(stems/ha) = \frac{\begin{array}{c}[(initialdensity + densityafter1stthinning)/2 + \\ \dfrac{\text{density after 1st thinning} + \text{density after 2nd thinning}}{2} + \cdots . \\ + (densitybeforelastthinning + densityafterlastthinning)/2]\end{array}}{\mathrm{n}}$$

Besides, b and ε denote random variables (stand types and trees) and residuals, respectively.

By using the "dredge" function from the "MuMin" package in R (Barton, 2010), we select the two best models (Eqns. (3), 4) for explaining the growth trend (Eqn. (3), and patterns (regularity and irregularity) (Eqn. (4) with crown shape variables. Also, we cross-checked the models performance by "performance" package in R (Lüdecke et al., 2021).

$$cutrw_{ij} = a_o + a_1 year \times (ca + cratio + cslc + th + cvcr + hmaxcr + maxcr) + b_i + \varepsilon_{ij} \quad (3)$$

$$cvtrw_{ij} = a_o + a_1 ca_{ij} + a_2 cvcr_{ij} + a_3 cslc_{ij} + b_i + \varepsilon_{ij} \quad (4)$$

Even though the effects of SDI were tested, they were excluded from the final models because the effects SDI on the relationships was not significant.

To predict internal growth patterns by using crown shape parameters (HIII), we used the β-crown shape traits (ca, cb) (Eqn. (5), 6) and compared them across competition gradients.

$$\log(\mathrm{cutrw}) = \mathrm{a_0} + \mathrm{a_1\ year} \times (\mathrm{ca}) + \mathrm{a_2}(1|\mathrm{tree_{id}}) \quad (5)$$

$$\log(\mathrm{trw}) = \mathrm{a_0} + \mathrm{a_1\ year} \times (\mathrm{ca} + \mathrm{cb}) + \mathrm{a_2}(1|\mathrm{tree_{id}}) \quad (6)$$

where trw, cutrw, ca, and cb indicate tree ring width, cumulative tree ring width, beta first, and beta second crown shape parameters, respectively.

We also demonstrated the potential use of machine learning (ML) applications in the quantitative correlations between crown and tree ring patterns and internal pattern prediction from external crown shape, employing random forest regressors (RFR), k-nearest neighbor (KNN), support vector regressors (SVR), and artificial neural networks (ANN) by using the "randomForest", "class," "e1071," 'neuralnet" packages in R, respectively (Fritsch et al., 2019; Liaw and Wiener, 2002; Meyer et al., 2019; Ripley et al., 2015). For each variable added to the input layer during the training of the ANNs, three neurons were used in the hidden layer. A logistic function is used in the hidden layer, while a linear function is used in the output layer by following Bueno et al. (2022). To increase the model's clarity, we only used and applied significant influencing crown variables that were observed in linear mixed models (Eqns. (3) and (4). To apply machine learning algorithms, we first purposefully increase the size of the dataset due to its nonlinear behavior. Dividing small (in our case, 30) datasets into training, testing, and validation datasets may increase the model uncertainties and chance of overfitting. We therefore added 300 additional random datasets through data augmentation (bringing the total to 330) based on the mean and standard deviation of the datasets. We then used 60% of the dataset for model training and the remaining 40% for both testing and validation.

In addition, to validate the models and check how variability in crown shape affects the growth curve and competition reduction influences the crown shape, we simulated 50-year crown shape and growth curve development with density gradients (SDI). The simulation was based on allometric relationships that estimated tree height (h), crown base height (cbh), and crown radius (cr) based on tree diameter (d) and tree age. The double-logarithmic relationship was used to model these relationships, and the data from repeated surveys was used to fit the model to the data using the simulation methods from Pretzsch et al. (2022).

All statistical analyses were done in the R environment (version 4.2.1, www.r-project.org).

3. Results

3.1. Relationships between crown shapes and tree ring patterns (HI)

The shape of the β-crown parameter (ca corresponds to crown width) significantly influences the first β-parameter of the tree rings (ta corresponds to ring width), as shown in Fig. 2a and 2b. The second parameters (i.e., cb and tb) of the crown and tree rings are only slightly correlated. In addition, the metrics for crown and tree ring regularity or irregularity show a significant correlation (Fig. 2c). Changes in crown distribution also affect the distribution of tree rings, and higher crown slopes (which are produced by narrower crowns) result in more

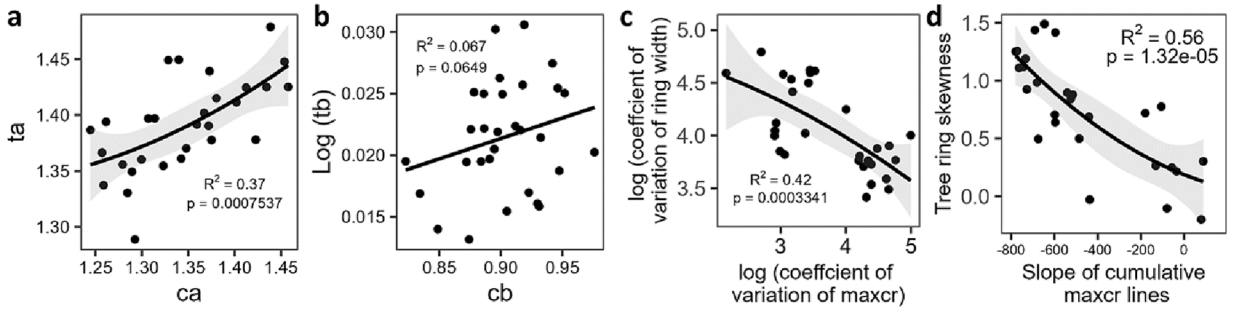

Fig. 2. Relationships between crown shape and tree ring pattern metrics. (a–b) the crown shape and tree ring patterns explaining β-parameters. (b) Crown regularity vs. tree ring regularity, and (c) tree ring skewness vs. crown slopes or angles. Besides ca, cb, and ta, tb refers to beta crown and tree ring shape parameters, while maxcr indicates maximum crown radius at each 5 cm crown length.

asymmetric tree rings ($p < 0.05$), as demonstrated by the strong association between tree ring skewness and the slope of the corresponding tree crown profile (which is exposed to the sun) in our slope-based regression analysis (Fig. 2d).

We found through simulation that the variation in crown shape strongly affects tree ring patterns (i.e., cumulative growth) (Fig. 3). We initially identified paraboloid, cone, and neiloid crown shapes in spruce trees (Fig. 3a–c), and then evaluated the effect of crown shape on radial growth patterns by tree ring (Fig. 3d). We also found that a wider crown produces a wider ring or higher radial growth. For example, the growth patterns change in the following order: parabolic > conical > neilodal crown (Fig. 3a–c).

Our fitted linear mixed model demonstrates that the metrics of crown shape significantly influence tree ring growth and patterns (Table 2). In particular, the coefficients for crown slenderness and crown radius significantly influence tree ring patterns (Table 2). The total explanatory power of the cutrw (cumulative tree ring width) model is substantial (conditional $R_c^2 = 0.96$), with the part related to the fixed effects alone (marginal R_m^2) being 0.83. The total explanatory power of the cvtrw model is also strong ($R_c^2 = 0.76$), with the part related to the fixed effects alone (R_m^2) being 0.17 (Table 2). The difference between R_c^2 and R_m^2 indicates that the random effect is important and is explained by tree and stand types.

However, we observed that simulated crown shapes (based on density gradients) also showed that with increasing densities, slenderness coefficients increased, indicating that higher densities produced narrower tree crown shapes or vice versa (Supplementary Fig. 3).

3.2. Variation in crown shape and tree ring patterns across competition gradients (HII)

We found comparable crown profiles with tree ring patterns across density gradients and in thinned and unthinned stands, indicating that trees in lower density stands produce broader or larger crowns, which promote extended and transgressive tree ring growth (wider rings) compared to those in higher density and unthinned stands (compare Fig. 4a, b, c, and d, and Supplementary Fig. 4). However, the β-distributions showed that trees from low density or thinned stands produced more upper-reaching (i.e., maxcr shifted to the crown top) crowns than those in high density or unthinned stands (lower-reaching, with maxcr shifted to the live crown base) (Fig. 4e and Supplementary Fig. 5), while producing comparable crown and tree ring cumulative patterns with an initial upward shift that later terminated in the high density or unthinned crown and tree ring cumulative β-distributions (compare Fig. 4f-g and Supplementary Fig. 5).

Similar to the patterns, the crown shape parameters showed strong variation across density gradients (Fig. 5). The crown and tree ring β-shape parameters, particularly the first β-shape parameters for both the crown (ca) and tree rings (ta), decreased significantly in high-density or unthinned stands (Fig. 5a). In contrast to the β-shape parameters, the slenderness ratio increased with density, indicating that as density increased, the crown narrowed (Fig. 5b). In addition, the mean maximum crown radius (maxcr) (Fig. 5c) and height of maximum crown radius (hmaxcr) were highest in the low-density stands, indicating a wider and upper-reaching crown (with the crown volume shifted towards the mid-direction) in low-density stands. The irregularity of the crown, defined by the coefficient of crown radius, similarly increases in low-density stands. In contrast, the tree rings in high-density stands showed the most irregularities (see Fig. 5e and f).

3.3. Growth curve prediction from crown shape (HIII)

Our predicted growth curve as a function of β-crown shape parameters (ca, cb, which correspond to crown width and crown length,

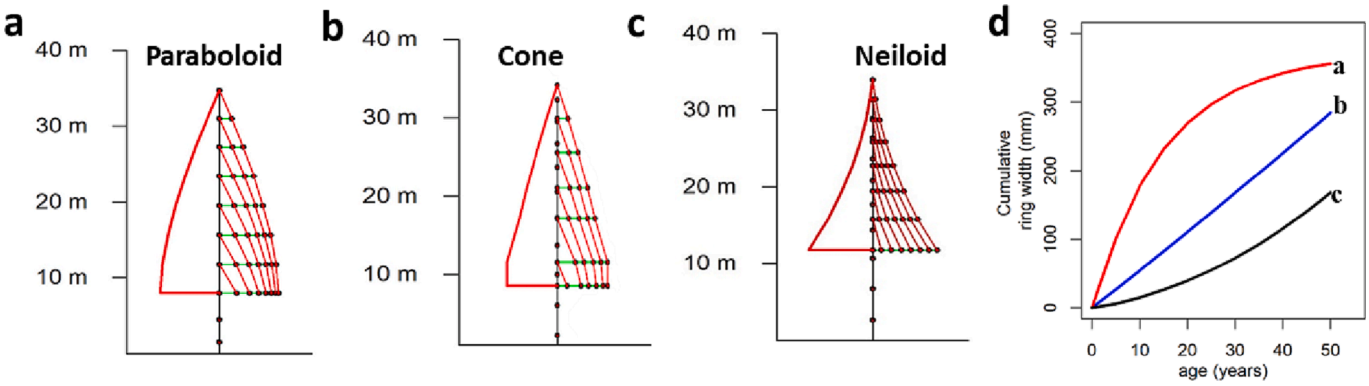

Fig. 3. Visualizes the simulated crowns with different crown shapes (a–c) (a: paraboloid, b: conical, c: neiloid). Corresponding simulated growth curves for simulated tree shapes (d).

Table 2
Summary of linear mixed models for analyzing the relationships between crown shape and tree ring pattern metrics. SD denotes the standard deviation. Besides, cutrw and cvtrw indicate the cumulative tree ring width and coefficient of variation of the tree ring with, respectively.

	cutrw			**cvtrw**		
Predictors	*Estimates*	*SD*	*p*	*Estimates*	*SD*	*P*
(Intercept)	9047.17	796.65	**<0.001**	200.61	36.9	**<0.001**
year	−45422.68	3972.8	**<0.001**			
th	−323.38	29.57	**<0.001**			
maxcrad	−2446.88	164.57	**<0.001**			
cvcr	2745.81	576.62	**<0.001**	58.28	23.5	**0.02**
ca	−2779.28	469.23	**<0.001**			
cratio	−1200.46	176.4	**<0.001**	−19.44	7.85	**0.021**
year * th	1636.83	147.45	**<0.001**			
year * maxcrad	12314.62	820.72	**<0.001**			
year * cvcr	−13795.57	2876.1	**<0.001**			
year * ca	13956.62	2340.2	**<0.001**			
year * cratio	6053.84	879.85	**<0.001**			
cw						
cslc				−4.82	1.21	**0.001**
Random Effects						
σ^2	95.4			202.46		
τ_{00}	293.40 $_{tree\_id:type}$			497.29 $_{tree\_id:type}$		
ICC	0.75			0.71		
N	30 $_{tree\_id}$			30 $_{tree\_id}$		
	2 $_{type}$			2 $_{type}$		
Marginal R^2/Conditional R^2	0.830/0.958			0.167/0.759		

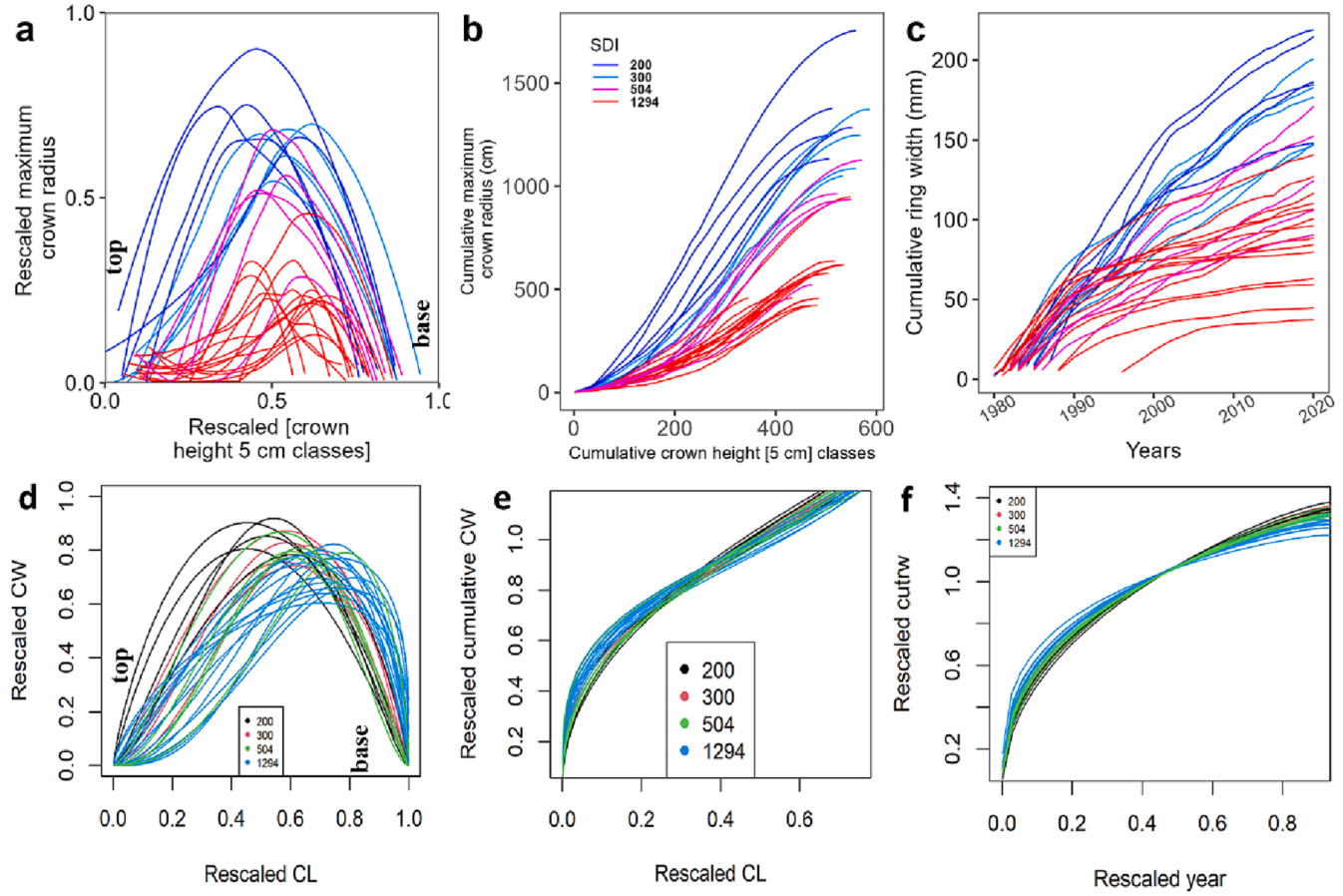

Fig. 4. Visualizing changes in crown profiles and tree ring patterns across density gradients. (a) Crown profile (divided height classes of 0.05 cm against the maximum crown radius, maxcr); (b) cumulative maxcr; and (c) cumulative tree ring width patterns (cutrw). (d–f) Visualizing β crown and tree ring distributions across density gradients. (e) β-distribution fitted to crown profiles (CW-crown width and CL-crown length), (f) β-cumulative CW and CL distributions, and (g) β-cumulative tree ring patterns (cutrw-cumulative tree ring width and years). The figure represents the crown shape and ring patterns of 30 different trees.

respectively) produced comparable results while distinguishing between competition gradients (Fig. 6a, d, and Table 3). The model also predicts that in low-density or less-competitive stands, wider crowns (indicated by higher β-shape values) can be found, indicating higher growth than those in high-competitive stands (Supplementary Fig. 6). It is clear from the comparative growth projections that growth patterns increase as the

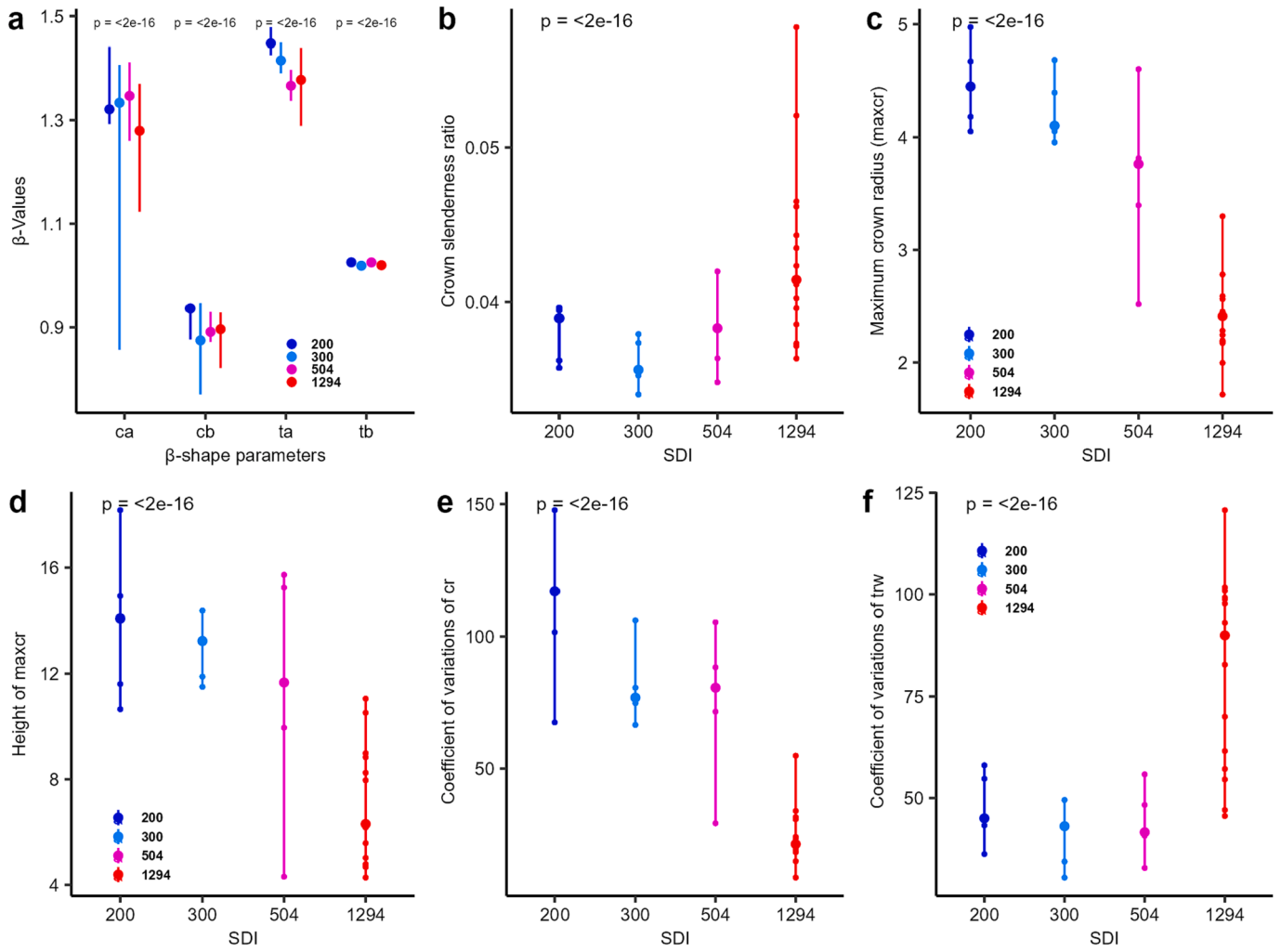

Fig. 5. Visualizes the variations in crown shape and tree ring patterns across a density gradient: (a) variation in β-crown shape and tree ring pattern parameters; (b) crown slenderness ratio; (c) maximum crown radius (maxcr); (d) maximum crown radius height (hmaxcr); (e) coefficient of variation of crown radius (cvcr); (f) coefficient of variation of tree ring width (cvtrw). the vertical lines show a 95% confidence interval, and the solid, larger circles indicate mean values, while each point denotes the mean values for each tree. The p-value indicates the level of significance (adopted from the one-way anova).

crown β (ca) values rise. The accuracy analysis of the model (i.e., observed vs. predicted) indicates that crown shape parameters can be used to predict internal growth patterns with higher accuracy (RMSE = 0.38–0.54 and R^2 = 0.72–0.41) (Fig. 6c and f).

In this study, we explored the potential of machine learning (ML) techniques to advance our understanding of the relationship between crown shape and tree ring patterns. To do this, we applied four commonly used ML algorithms to predict tree ring patterns based on crown shape variables. Our results showed that these approaches were capable of linking and predicting tree ring patterns and growth metrics. We also found that increasing the number of crown variables can improve the performance of the models (Table 4).

In addition to the overall success (low RMSE, MAP, and MAPE values) of machine learning in predicting tree ring patterns, our comparative results showed that the random forest regressor (RFR) and the k-nearest neighbor (KNN) ML approaches had the best performance among the four machine learning techniques we used. This was reflected in both the results in Table 4 and the comparative validation curve in Fig. 7.

4. Discussion

Understanding the underlying mechanisms that will allow us to predict how trees will grow in the future is critical to growth modeling. Here, we aimed to simplify (through complex evaluations) and improve the quantitative understanding by disentangling the relationships between tree ring patterns and crown shape (regularity vs. irregularity) across density or competition gradients. These results are important for understanding how trees grow on the inside while their shape changes on the outside at different levels of competition.

4.1. Link between crown shape and tree ring patterns across competition gradients

To understand many underlying mechanisms, especially the cause of changing 3D patterns of crown development, shape, and function along tree ring patterns, is critical but remains mostly unsolved (Bohn and Huth, 2017; O'Sullivan et al., 2021). We therefore tried to link 3D crown shape (CS) to tree ring patterns and observed that CS explaining variables and tree ring pattern (TRP) metrics were significantly correlated, while crown irregularity strongly defines tree ring irregularity and growth (Fig. 2, Table 2). We expected that crown and tree ring patterns (coefficient of variation of crown radius (cvcr) vs. tree ring width (cvtrw)) would be positively correlated, but overall data (bivariate relationship) demonstrated negative relationships (Fig. 2c), while mixed models identified positive relationships between cvcr and cvtrw (Table 2). We reasoned that defining relationships between CS and TRP at the individual tree level is critical (see R^2_m vs. R^2_c) and indicates that CS

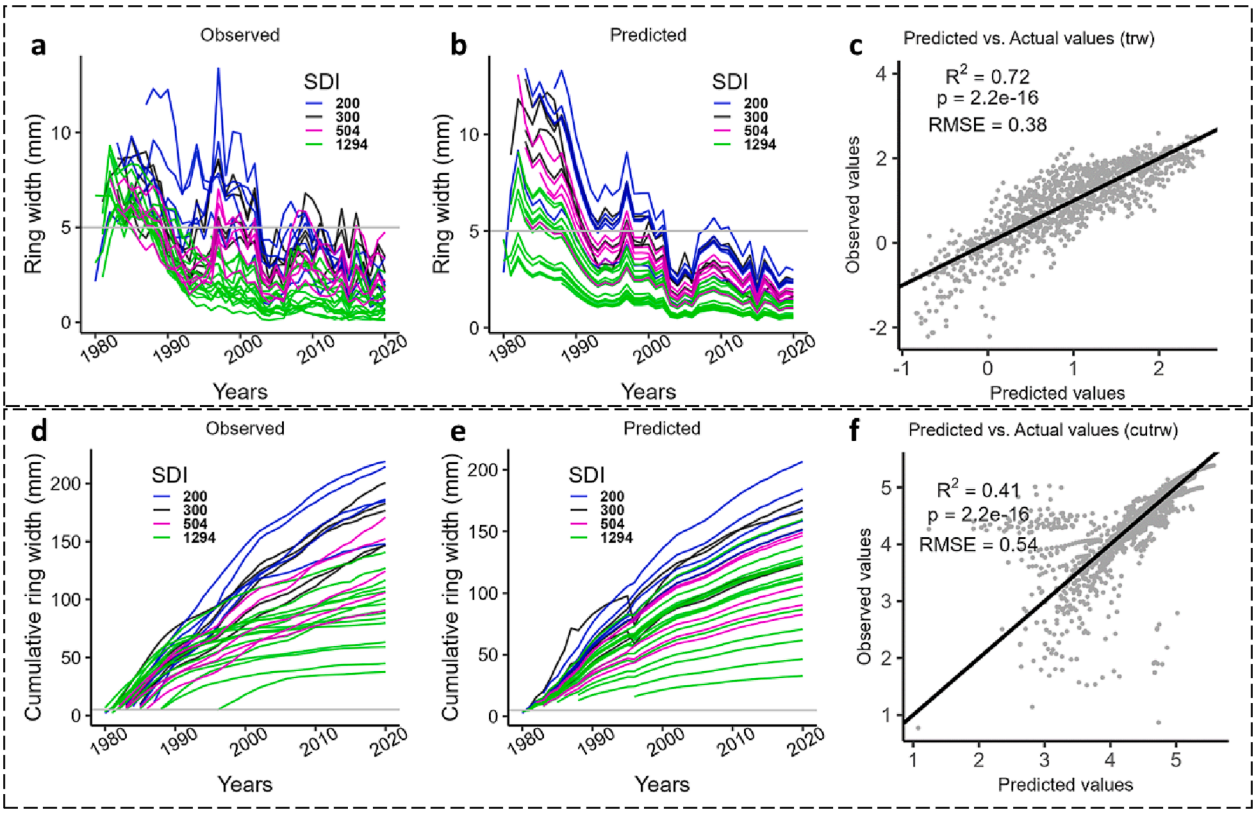

Fig. 6. Shows the growth curve prediction as a function β-crown shape parameter (ca and cb). (a) Observed and (b) predicted tree ring inter annual variability prediction across density gradients, respectively. (c) The actual vs. predicted plot fortree ring width (trw). (d–e) Observed and predicted cumulative tree ring patterns across density gradients, respectively. (c) The actual vs. predicted plot for cumulative tree ring width (cutrw), SDI, and RMSE denote the stand density index and root mean square error, respectively.

Table 3
Details model predictions summary for cumulative tree ring width (cutrw) and tree ring with (trw). CI denotes 95% confidence interval. Where ca and cb indicate beta crown shape parameters, respectively.

	log(cutrw)			**log(trw)**		
Predictors	*Estimates*	*CI*	*p*	*Estimates*	*CI*	*P*
(Intercept)	96.74	26.84 – 166.64	**0.01**	−158.71	−280.32 – -37.10	**0.011**
year [log]	57.97	14.53 – 101.41	**0.01**			
ca	54.95	0.90 – 108.99	**0.05**	−189.8	−257.32 – -122.27	**<0.001**
year [log] * ca	33.83	0.24 – 67.41	**0.05**			
year				796.43	189.28 – 1403.58	**0.01**
cb				553.99	356.53 – 751.45	**<0.001**
year * ca				953.87	616.85 – 1290.89	**<0.001**
year * cb				−2774.65	−3760.31 – -1788.99	**<0.001**
Random Effects						
σ^2	0.13			0.21		
τ_{00}	0.14 $_{tree\_id}$			0.30 $_{tree\_id}$		
ICC	0.52			0.58		
N	30 $_{tree\_id}$			30 $_{tree\_id}$		
Observations	1124			1124		
Marginal R^2/Conditional R^2	0.534/0.774			0.339/0.724		

and TRP strongly vary at the tree level. Furthermore, the slope (steepness) of the same tree's crown profile and tree ring skewness (level of asymmetry) are statistically correlated (Fig. 2c), indicating that a narrower crown is more likely to produce asymmetric TRP. Narrower crown indicates that if a tree's crown growth is getting narrower, it is a sign that the tree has been experiencing some sort of resource limitation, such as insufficient access to nutrients, water, sunlight, etc. that it required to grow at a consistent rate due to a high level of competition, resulting in an irregular pattern of growth in the tree's rings, with some being wider and others being narrower. However, the level of regularity or irregularity could be varied between crown shapes (e.g., paraboloid, cone, neiloid, etc.) as well, which might strongly influence the tree ring growth patterns. For example, our simulation demonstrated that trees with paraboloid crowns (relatively regular) grow faster, which indicates a wider ring than conical and neiloid crowns (Fig. 3a-c). This suggests a strong link between crown shape and tree ring patterns and is identical to the prior results of Pretzsch et al. (2022). Changes in crown shapes indicate the loss or gain of photosynthetic areas, which strongly influence the photosynthesis rate and subsequent growth. Besides, our findings suggest that the variations in the crown size and shape could be due to growing conditions (in our case, density differences or level of competition) and support the hypothesis of Pretzsch et al. (2022), where

Table 4
Comparative results of machine learning approaches to predict internal tree ring patterns (coefficient of variation of tree ring patterns, cvtrw) from crown shape variables. KNN, RFR, SVR, and ANN indicate the k-nearest neighbor, random forest regressor, support vector regressor, and artificial neural network, respectively. RMSE, MAP, and MAPE denote root mean square errors, mean absolute error, and mean absolute error, respectively. See Table 1 for the full forms of the variables that are used for the analyses.

Model	ML approach	Model Input	R^2	RMSE	MAE	MAPE
1	KNN	cr, cl, th, cvcr, cratio, maxcr, hmaxcr, ca, cb	**0.94**	**5.35**	**2.97**	**0.05**
	SVR	cr, cl, th, cvcr, cratio, maxcr, hmaxcr, ca, cb	0.51	15.51	9.54	0.13
	RFR	cr, cl, th, cvcr, cratio, maxcr, hmaxcr, ca, cb	**0.95**	**4.83**	**2.09**	**0.03**
	ANN	cr, cl, th, cvcr, cratio, maxcr, hmaxcr, ca, cb	0.63	14.73	12.13	0.2
2	KNN	cr, th, cvcr, cratio, maxcr, hmaxcr, ca, cb	**0.95**	**4.97**	**2.92**	**0.05**
	SVR	cr, th, cvcr, cratio, maxcr, hmaxcr, ca, cb	0.61	13.74	8.63	0.12
	RFR	cr, th, cvcr, cratio, maxcr, hmaxcr, ca, cb	**0.97**	**4.09**	**2.33**	**0.04**
	ANN	cr, th, cvcr, cratio, maxcr, hmaxcr, ca, cb	0.59	14.89	11.93	0.19
3	KNN	cr, th, cvcr, cratio, maxcr, ca, cb	0.82	9.69	4.43	0.07
	SVR	cr, th, cvcr, cratio, maxcr, ca, cb	0.49	16.85	11.87	0.17
	RFR	cr, th, cvcr, cratio, maxcr, ca, cb	0.9	6.8	3.84	0.06
	ANN	cr, th, cvcr, cratio, maxcr, ca, cb	0.62	15.15	12.21	0.21
4	KNN	cr, th, cvcr, cratio, maxcr, ca	0.82	9.61	4.45	0.07
	SVR	cr, th, cvcr, cratio, maxcr, ca	0.5	16.78	11.55	0.16
	RFR	cr, th, cvcr, cratio, maxcr, ca	0.9	6.69	3.76	0.06
	ANN	cr, th, cvcr, cratio, maxcr, ca	0.62	15.24	12.5	0.21
5	KNN	cr, cvcr, cratio, maxcr, ca	0.63	13.16	8.93	0.12
	SVR	cr, cvcr, cratio, maxcr, ca	0.5	16.78	11.55	0.16
	RFR	cr, cvcr, cratio, maxcr, ca	0.65	12.27	8.2	0.12
	ANN	cr, cvcr, cratio, maxcr, ca	0.63	14.18	11.24	0.18
6	KNN	cvcr, maxcr, ca	0.57	14.33	10.52	0.15
	SVR	cvcr, maxcr, ca	0.16	22.37	15.59	0.2
	RFR	cvcr, maxcr, ca	0.65	12.27	8.2	0.12
	ANN	cvcr, maxcr, ca	0.62	14.93	11.86	0.19

the authors predicted that trees growing in open conditions may tend to produce a paraboloidal-shaped crown. In contrast, trees in higher competition conditions are likely to produce a conical to neiloid crown shape, while they hypothesized that four basic crown shapes can be observed in Norway spruce, including an irregular crown shape. However, identifying the irregular crown shape precisely is a contentious issue, albeit, simple to measure the degree of regularity (less or more) using the proxy variables of the coefficient of crown radius (cvcr) (a larger cvcr value indicates more irregularity). In addition to growing conditions (degree of competition) (Kuprevicius et al., 2013), crown complementarity (level of dominance), neighboring tree characteristics, species richness (Pretzsch and Rais, 2016; Pretzsch and Schütze, 2009), and largely by species identity (Pyörälä et al., 2019), might work underneath to define the CS, which could potentially influence TRP. However, we were unable to detect how CS and TRP are changing with dominance and suppressed characteristics (as our dataset was only from even-aged stands). So, future research should focus on how crown shape and tree ring patterns vary across levels of dominance.

Furthermore, our mixed models depicted that stand density index (SDI) had no significant influence on the link between crown shape and tree ring pattern metrics (Fig. 5a-c). This neutral result could be attributed to the simultaneous effect of competition on crowns and tree rings, indicating that increasing density or level of competition reduces crown shape and tree ring size at the same time. In contrast, SDI separately impacts crown shape parameters (Fig. 3), indicating that higher density reduces the shape parameters for the crown and tree ring. Our randomly picked and simulated trees from four density gradient plots (Supplementary Fig. 1) also showed that with increasing density, crown shape got narrower (Supplementary Fig. 3).

4.2. Crown shape and tree ring patterns variation across competition gradients

The tree ring patterns trees formed were comparable with crown shape (CS) patterns across competition levels (see Fig. 4a-d). Our observed comparable patterns denote that tree ring patterns (TRP) strongly reflect sufficient information in the corresponding tree's crown shape. Thinning or competition reduction had a strong impact on tree TRP (Donfack et al., 2022) and CS (this study), indicating that while the crown profile changes with spacing or density reduction, TRP also changes comparably (Fig. 4 and Supplementary Figs. 4 and 5). Several studies already confirmed that thinning caused transgressive stem growth patterns (Pretzsch, 2005), while here we found comparative and transgressive crown growth in less-dense stands than denser stands (see Figs. 4 and 5), compared to unthinned or highly dense stands. Furthermore, in less dense stands, β-crown shape based tree ring development denotes higher growth than unthinned stands, indicating that a wider crown and higher growth are mutually exclusive (Fig. 4e-g). Reduced density (through thinning or initial spacing), increased available growing space and resources (above and belowground), and reduced interspecific competition (Owen et al., 2021; Saarinen et al., 2022) could have promoted a larger crown. This relationship can also be generalized by concluding that big trees with larger crowns add more carbon to stems than trees with small crowns (Stephenson et al., 2014), although the higher growing space requirements for large trees may reduce the growth (Sillett et al., 2015), while thinning may sharply increase the growth (Pretzsch, 2005). We, however, noticed that crown irregularity (coefficient of variation of crown radius, cvcr) increased with decreasing density, possibly due to thinning and the necessity of stability against winds as thinning creates space, which accelerates crown expansion according to available light direction, or crown stabilizing mechanisms might work underneath. A few studies have already discussed that thinning exposed trees to wind and resulted in increased diameter growth as resistance mechanism (Donfack et al., 2022; Gardiner and Brüchert, 2006), indicating more stability in tree base. Similarly, we found a low coefficient of variation in tree rings (cvtrw), i.e., a low cvtrw value in low-density stands, denoting more regular or stable tree ring patterns and regularity, which may likely continue to crown after securing tree ring stability. As Donfack et al. (2022) predicted, crown stability (more regular patterns) can be secured once stem base stability is secured through carbon accumulation at the tree bases. Besides, crown vitality (healthiness) could also play a critical role in defining crown regularity level by avoiding crown damage. For example, Drobyshev et al. (2007) found a link between crown condition and tree ring size in Swedish oak (*Quercus robur*), noting that healthy crowns created a larger tree ring than deteriorated crowns. Branch damage leads to changes in crown structure by decreasing crown ratio

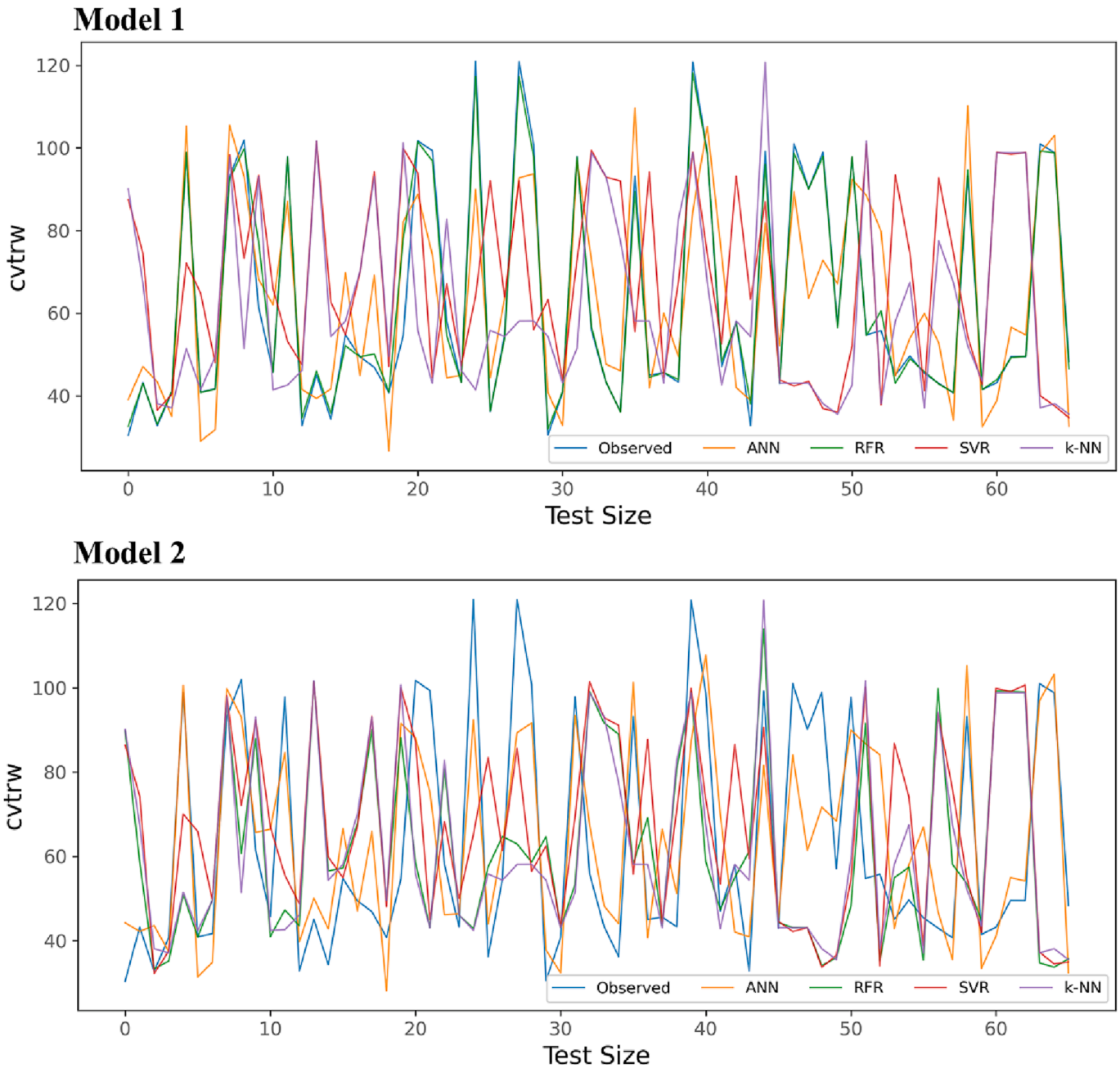

Fig. 7. Visualizing and comparing the first (Model 1) and second (Model 2) best-fitting machine learning models KNN, RFR, SVR, and ANN indicate k-nearest neighbor, random forest regressor, support vector regressor, and artificial neural network, respectively. The rest of the models are presented in Supplementary Fig. 7. cvtrw is the coefficient of variation of tree ring width in percentage. Test size is the number of simulated data used for testing (in this case, 66 samples).

(Mäkelä and Valentine, 2006), which could also produce irregular crowns. In addition, crown damage reduces photosynthesis capability and increases tree mortality, which thereafter effects growth and carbon cycling (McDowell et al., 2008; Needham et al., 2022). Thus, we expect crown damage or loss might affect crown shape and tree ring patterns in low-density stands. By contrast, higher irregularity in tree rings in dense or unthinned stands could also be explained by stronger competition for resources, a lower stability requirement, or both.

Furthermore, we observed through the β-distributions that an unthinned stand produced a lower-reaching crown, while a thinned stand produced a more upper-shifted crown profile (Fig. 4e), indicating crown volume shifted to a lower crown with increasing density. Similarly, Barbeito et al. (2017) found that crown volume for *F. sylvatica* in mixed stands shifted to a lower crown part (i.e., lower-reaching) compared with pure stands. Such results denote mixing and stand density had a significant impact on crown expansion, though the relationship between crown shape and tree ring patterns in mixed stands remains unknown. Besides, CS and TRP showed comparable patterns, resulting in less dense stands producing more upward-dispersed cumulated tree rings (a higher vegetation period) compared to tree rings in an unthinned stand (growth terminating at a later stage) (Fig. 4f–g), indicating neighboring competition plays a critical role in defining CS and TRP metrics and growth. Furthermore, promoting crown development through thinning may promote a more complex crown shape and growth functions (Deleuze et al., 1996), which could have also increased the tree ring irregularity in less dense stands. Therefore, it may be worthwhile to mention that with a variety of silvicultural practices, this connection and variations in crown can critically alter growth trends

(Martin-Ducup et al. (2020); and see Fig. 4).

4.3. Growth curve development from crown shape across competition gradients

Growth prediction can improve the understanding of ecophysiological and statistical modeling (Mäkelä and Valentine, 2006). Overall, this understanding may help to manage forests sustainably in an improved way (Pretzsch et al., 2022). Prior and conventional growth prediction approaches were based on tree age and total mass (discussed in Pretzsch (2021b)), while growth prediction from the crown is rarely focused. However, adding crown variables (e.g., crown projection area) to the growth model improves the models (discussed in the introduction section). To combine and understand ecophysiological and statistical models, we predict growth patterns based solely on crown shape, explaining statistical metrics (here, β-shape parameters) that resulted in comparable growth patterns across density gradients (Table 2; compare Fig. 6a-b and d-e). To simplify the model, we initially included all significant crown variables (Eqns. 2), which produced roughly identical models to the observed models; thus, the exclusion of other variables was done. Our model predictions are significant and highly accurate (see RMSE) (Fig. 6c and f), and the inclusion of second β-crown shape parameter (cb) in the model increased the accuracy level when predicting raw tree ring widths by 23% (Fig. 6f). Indicating the shape parameter can explain sufficient information about growth traits (current and future growth). This result suggests that in addition to the growth curve prediction, we can also predict inter-annual variability from the crown shape. However, by covering more crown shapes from diverse stands, we may get better information. Therefore, more study is required to examine the statistical links between internal and external variables. In order to better comprehend the growth model, we need critical evaluation to understand the mathematical crown shape, its variations, and how changes in the crown shape affect tree ring patterns and growth. In addition to simple approaches, prior research in quantitative understanding of the relationships between crown structure and growth, i.e., Pretzsch et al. (2022), assumed these relationships could be quantified with advanced methods such as machine learning (ML). We applied ML techniques to predict tree ring patterns based on crown shape variables. The random forest regressor (RFR) approach performed the best among the four ML techniques we used, explaining about 97% of the diverse associations between crown shape and tree ring pattern variables (Table 4, Model 2). These findings suggest that RFR and KNN (k-nearest neighbors) ML approaches are effective in predicting tree ring patterns (see Table 4 and Fig. 7) and may be useful for further study. In terms of accuracy, linear mixed models outperformed ML approaches (compare the RMSE values: mixed model RMSE of 3.8% and the lowest RMSE for RFR of 4.09) while comparing Table 4 and Fig. 4. While data augmentation using the mean and standard deviation could lessen the uncertainties, ML techniques might benefit from augmented datasets (330) than a linear mixed modeling approach (which employed only 30). However, our study was limited by a small dataset of only 30 trees, so a larger and more robust dataset is recommended for future applications. Despite this limitation, our findings suggest that ML approaches can be a valuable tool in advancing the study of tree ring patterns and crown shape relationships. It has the potential to provide new insights and help us better understand the complex processes that drive tree growth and development. As such, it has the potential to inform conservation and management efforts aimed at protecting and promoting the health of forests and ecosystems through ecological modeling and tree health analysis.

5. Conclusions

Our study found a strong relationship between crown shape and tree ring patterns. Changes in crown shape can affect tree growth and the patterns of tree rings. We observed that the slopes and volume distribution of the crown have a significant impact on tree ring patterns, e.g., with upward-reaching crowns having higher growth and larger rings. We also found that stand density or level of competition can simultaneously impact crown and tree ring growth, with density reduction improving both. Therefore, this study provides the basis for understanding how density (increasing or decreasing) affects the 3D structure of trees, followed by the internal growth patterns. Several approaches, ranging from simple to advanced, can be used to quantitatively account for the relationships between crown shape and tree ring patterns. For example, machine learning (ML) approaches can be used to predict internal ring patterns from external shape patterns along with simple linear models. Our methodological study only evaluated a limited dataset, so further research is needed to understand the relationship between CS and TRP in different species. A larger dataset and the use of ML techniques may provide additional insights into these relationships. Our finding suggests that quantifying the shape of a tree's crown and tree ring patterns is critical for advancing ecological modeling and improving our understanding of the tree's growth efficiency, as well as potentially improving silvicultural prescriptions.

CRediT authorship contribution statement

Shamim Ahmed: Conceptualization, Data curation, Formal analysis, Methodology, Writing – original draft. **Hans Pretzsch:** Conceptualization, Writing – review & editing.

Declaration of Competing Interest

The authors declare that they have no known competing financial interests or personal relationships that could have appeared to influence the work reported in this paper.

Data availability

Link shared

Acknowledgements

The authors would like to thank their colleagues Martin Jacobs, Luke Bohnhorst, Gerhard Schmied, and Martin Honold for their assistance in collecting and sharing TLS and dendrochronological data. We also appreciate the help Enno Uhl and Torben Hilmers provided during the concept-development process. We would like to thank Dr. Peter Biber and Chien Chen, Chair of Forest Growth and Yield Science, and Minhaz Rahman, TUM School of Life Sciences, Technical University of Munich (TUM), who helped us during data analysis in R.

Funding

This work is funded by European Union's Horizon 2020 research and innovation program under Marie Skłodowska-Curie Grant Agreement No. H2020-MSCA-ITN-2020-956355.

Appendix A. Supplementary data

Supplementary data to this article can be found online at https://doi.org/10.1016/j.ecolind.2023.110116.

References

Anderson-Teixeira, K.J., McGarvey, J.C., Muller-Landau, H.C., Park, J.Y., Gonzalez-Akre, E.B., Herrmann, V., Bennett, A.C., So, C.V., Bourg, N.A., Thompson, J.R., 2015. Size-related scaling of tree form and function in a mixed-age forest. Funct. Ecol. 29, 1587–1602.

Antin, C., Pélissier, R., Vincent, G., Couteron, P., 2013. Crown allometries are less responsive than stem allometry to tree size and habitat variations in an Indian monsoon forest. Trees 27, 1485–1495.

Antonarakis, A.S., Richards, K.S., Brasington, J., Muller, E., 2010. Determining leaf area index and leafy tree roughness using terrestrial laser scanning. Water Resour. Res. 46.
Arslan, A.E., Erten, E., Inan, M., 2021. A comparative study for obtaining effective Leaf Area Index from single Terrestrial Laser Scans by removal of wood material. Measurement 178, 109262.
Barbeito, I., Dassot, M., Bayer, D., Collet, C., Drössler, L., Löf, M., del Rio, M., Ruiz-Peinado, R., Forrester, D.I., Bravo-Oviedo, A., 2017. Terrestrial laser scanning reveals differences in crown structure of Fagus sylvatica in mixed vs. pure European forests. For. Ecol. Manage. 405, 381–390.
Barton, K., 2010. MuMIn: multi-model inference. R package version 0.13. 17. http://CRAN. R-project. org/package=MuMIn.
Bates, D.M., 2010. lme4: Mixed-effects modeling with R. Springer, New York.
Bayer, D., Seifert, S., Pretzsch, H., 2013. Structural crown properties of Norway spruce (Picea abies [L.] Karst.) and European beech (Fagus sylvatica [L.]) in mixed versus pure stands revealed by terrestrial laser scanning. Trees 27, 1035–1047.
Bohn, F.J., Huth, A., 2017. The importance of forest structure to biodiversity–productivity relationships. R. Soc. Open Sci. 4, 160521.
Bueno, G.F., Costa, E.A., Finger, C.A.G., Liesenberg, V., Bispo, P.D.C., 2022. Machine Learning: Crown Diameter Predictive Modeling for Open-Grown Trees in the Cerrado Biome. Brazil. Forests 13, 1295.
Bunn, A.G., 2008. A dendrochronology program library in R (dplR). Dendrochronologia 26, 115–124.
Calders, K., Adams, J., Armston, J., Bartholomeus, H., Bauwens, S., Bentley, L.P., Chave, J., Danson, F.M., Demol, M., Disney, M., 2020. Terrestrial laser scanning in forest ecology: Expanding the horizon. Remote Sens. Environ. 251, 112102.
Chaturvedi, R.K., Raghubanshi, A.S., Singh, J.S., 2011. Plant functional traits with particular reference to tropical deciduous forests: A review. J. Biosci. 36, 963–981.
Chhin, S., Hogg, E.H., Lieffers, V.J., Huang, S., 2010. Growth–climate relationships vary with height along the stem in lodgepole pine. Tree Physiol. 30, 335–345.
Corner, E.J.H., 1949. The durian theory or the origin of the modern tree. Ann. Bot. 13, 367–414.
del Río, M., Bravo-Oviedo, A., Ruiz-Peinado, R., Condés, S., 2019. Tree allometry variation in response to intra-and inter-specific competitions. Trees 33, 121–138.
Deleuze, C., Hervé, J.-C., Colin, F., Ribeyrolles, L., 1996. Modelling crown shape of Picea abies: spacing effects. Can. J. For. Res. 26, 1957–1966.
Donfack, L.S., Schall, P., Mund, M., Knohl, A., Ammer, C., 2022. Effects of competition reduction on intra-annual radial growth of European beech (Fagus sylvatica L.) at stem base and crown base. Trees.
Drobyshev, I., Linderson, H., Sonesson, K., 2007. Relationship between crown condition and tree diameter growth in southern Swedish oaks. Environ. Monit. Assess. 128, 61–73.
Enquist, B.J., West, G.B., Charnov, E.L., Brown, J.H., 1999. Allometric scaling of production and life-history variation in vascular plants. Nature 401, 907–911.
Enquist, B.J., Allen, A.P., Brown, J.H., Gillooly, J.F., Kerkhoff, A.J., Niklas, K.J., Price, C. A., West, G.B., 2007. Does the exception prove the rule? Nature 445, E9–E10.
Esser, M.H.M., 1946. Tree trunks and branches as optimum mechanical supports of the crown: I. The trunk. Bull. Math. Biophys. 8, 65–74.
Franceschi, E., Moser-Reischl, A., Rahman, M.A., Pauleit, S., Pretzsch, H., Rötzer, T., 2022. Crown Shapes of Urban Trees-Their Dependences on Tree Species, Tree Age and Local Environment, and Effects on Ecosystem Services. Forests 13.
Fritsch, S., Guenther, F., Guenther, M.F., 2019. Package 'neuralnet'. Training of Neural Networks.
Gardiner, B.A., Brüchert, F., 2006. The effect of wind exposure on the tree aerial architecture and biomechanics of Sitka Spruce (picea sitchenisis Bong.).
Givnish, T.J., 1988. Adaptation to sun and shade: a whole-plant perspective. Funct. Plant Biol. 15, 63–92.
Grote, R., Pretzsch, H., 2002. A model for individual tree development based on physiological processes. Plant Biol. 4, 167–180.
Hahsler, M., Piekenbrock, M., Doran, D., 2019. dbscan: Fast density-based clustering with R. J. Stat. Softw. 91, 1–30.
Hemery, G.E., Savill, P.S., Pryor, S.N., 2005. Applications of the crown diameter–stem diameter relationship for different species of broadleaved trees. For. Ecol. Manage. 215, 285–294.
Jacobs, M., Rais, A., Pretzsch, H., 2021. How drought stress becomes visible upon detecting tree shape using terrestrial laser scanning (TLS). For. Ecol. Manage. 489, 118975.
Jacobs, M., Hilmers, T., Leroy, B.M.L., Lemme, H., Kienlein, S., Müller, J., Weisser, W.W., Pretzsch, H., 2022. Assessment of defoliation and subsequent growth losses caused by Lymantria dispar using terrestrial laser scanning (TLS). Trees.
Julio Camarero, J., Gazol, A., Sangüesa-Barreda, G., Cantero, A., Sánchez-Salguero, R., Sánchez-Miranda, A., Granda, E., Serra-Maluquer, X., Ibáñez, R., 2018. Forest growth responses to drought at short-and long-term scales in Spain: squeezing the stress memory from tree rings. Front. Ecol. Evol. 6, 9.
Junttila, S., Hölttä, T., Puttonen, E., Katoh, M., Vastaranta, M., Kaartinen, H., Holopainen, M., Hyyppä, H., 2021. Terrestrial laser scanning intensity captures diurnal variation in leaf water potential. Remote Sens. Environ. 255, 112274.
Kalliovirta, J., Tokola, T., 2005. Functions for estimating stem diameter and tree age using tree height, crown width and existing stand database information. Silva Fennica 39, 227–248.
Kholdaenko, Y.A., Belokopytova, L.V., Zhirnova, D.F., Upadhyay, K.K., Tripathi, S.K., Koshurnikova, N.N., Sobachkin, R.S., Babushkina, E.A., Vaganov, E.A., 2022. Stand density effects on tree growth and climatic response in Picea obovata Ledeb. plantations. Forest Ecology and Management 519, 120349.
Köcher, P., Horna, V., Leuschner, C., 2012. Environmental control of daily stem growth patterns in five temperate broad-leaved tree species. Tree Physiol. 32, 1021–1032.
Kokaly, R.F., Asner, G.P., Ollinger, S.V., Martin, M.E., Wessman, C.A., 2009. Characterizing canopy biochemistry from imaging spectroscopy and its application to ecosystem studies. Remote Sens. Environ. 113, S78–S91.
Kramer, P., 2012. Physiology of woody plants. Elsevier.
Kuprevicius, A., Auty, D., Achim, A., Caspersen, J.P., 2013. Quantifying the influence of live crown ratio on the mechanical properties of clear wood. Forestry 86, 361–369.
Kuznetsova, A., Brockhoff, P.B., Christensen, R.H.B., 2017. lmerTest package: tests in linear mixed effects models. J. Stat. Softw. 82, 1–26.
Lecigne, B., Delagrange, S., Messier, C., 2018. Exploring trees in three dimensions: VoxR, a novel voxel-based R package dedicated to analysing the complex arrangement of tree crowns. Ann. Bot. 121, 589–601.
Lehnebach, R., Beyer, R., Letort, V., Heuret, P., 2018. The pipe model theory half a century on: a review. Ann. Bot. 121, 773–795.
Liaw, A., Wiener, M., 2002. Classification and regression by randomForest. R news 2, 18–22.
Lüdecke, D., Ben-Shachar, M.S., Patil, I., Waggoner, P., Makowski, D., 2021. performance: An R package for assessment, comparison and testing of statistical models. J. Open Source Software 6.
Lüttge, U., Hertel, B., 2009. Diurnal and annual rhythms in trees. Trees 23, 683–700.
Mäkelä, A., Valentine, H.T., 2006. Crown ratio influences allometric scaling in trees. Ecology 87, 2967–2972.
Martin-Ducup, O., Ploton, P., Barbier, N., Momo Takoudjou, S., Mofack, G., Kamdem, N. G., Fourcaud, T., Sonké, B., Couteron, P., Pélissier, R., 2020. Terrestrial laser scanning reveals convergence of tree architecture with increasingly dominant crown canopy position. Funct. Ecol. 34, 2442–2452.
McDowell, N., Pockman, W.T., Allen, C.D., Breshears, D.D., Cobb, N., Kolb, T., Plaut, J., Sperry, J., West, A., Williams, D.G., 2008. Mechanisms of plant survival and mortality during drought: why do some plants survive while others succumb to drought? New Phytol. 178, 719–739.
Metz, J., Seidel, D., Schall, P., Scheffer, D., Schulze, E.-D., Ammer, C., 2013. Crown modeling by terrestrial laser scanning as an approach to assess the effect of aboveground intra-and interspecific competition on tree growth. For. Ecol. Manage. 310, 275–288.
Meyer, D., Dimitriadou, E., Hornik, K., Weingessel, A., Leisch, F., Chang, C.-C., Lin, C.-C., Meyer, M.D., 2019. Package 'e1071'. R J.
Montoro Girona, M., Rossi, S., Lussier, J.-M., Walsh, D., Morin, H., 2017. Understanding tree growth responses after partial cuttings: A new approach. PLoS One 12, e0172653.
Muller-Landau, H.C., Condit, R.S., Harms, K.E., Marks, C.O., Thomas, S.C., Bunyavejchewin, S., Chuyong, G., Co, L., Davies, S., Foster, R., 2006. Comparing tropical forest tree size distributions with the predictions of metabolic ecology and equilibrium models. Ecol. Lett. 9, 589–602.
Needham, J.F., Arellano, G., Davies, S.J., Fisher, R.A., Hammer, V., Knox, R.G., Mitre, D., Muller-Landau, H.C., Zuleta, D., Koven, C.D., 2022. Tree crown damage and its effects on forest carbon cycling in a tropical forest. Global Change Biol. n/a.
Netzer, Y., Munitz, S., Shtein, I., Schwartz, A., 2019. Structural memory in grapevines: early season water availability affects late season drought stress severity. Eur. J. Agron. 105, 96–103.
O'Sullivan, H., Raumonen, P., Kaitaniemi, P., Perttunen, J., Sievänen, R., 2021. Integrating terrestrial laser scanning with functional–structural plant models to investigate ecological and evolutionary processes of forest communities. Ann. Bot. 128, 663–684.
Ogle, K., Barber, J.J., Barron-Gafford, G.A., Bentley, L.P., Young, J.M., Huxman, T.E., Loik, M.E., Tissue, D.T., 2015. Quantifying ecological memory in plant and ecosystem processes. Ecol. Lett. 18, 221–235.
Olivier, M.-D., Robert, S., Fournier, R.A., 2016. Response of sugar maple (Acer saccharum, Marsh.) tree crown structure to competition in pure versus mixed stands. For. Ecol. Manage. 374, 20–32.
Owen, H.J.F., Flynn, W.R.M., Lines, E.R., 2021. Competitive drivers of interspecific deviations of crown morphology from theoretical predictions measured with Terrestrial Laser Scanning. J. Ecol.
Pearl, J.K., Keck, J.R., Tintor, W., Siekacz, L., Herrick, H.M., Meko, M.D., Pearson, C.L., 2020. New frontiers in tree-ring research. The Holocene 30, 923–941.
Poorter, L., Bongers, L., Bongers, F., 2006. Architecture of 54 moist-forest tree species: traits, trade-offs, and functional groups. Ecology 87, 1289–1301.
Poorter, L., Lianes, E., Moreno-de Las Heras, M., Zavala, M.A., 2012. Architecture of Iberian canopy tree species in relation to wood density, shade tolerance and climate. Plant Ecol. 213, 707–722.
Pressler, M.R., 1865. gesetz der stammbildung und dessen forstwirthschaftliche bedeutung insbesondere für den waldbau höchsten reinertrago.
Pretzsch, H., 2005. Stand density and growth of Norway spruce (Picea abies (L.) Karst.) and European beech (Fagus sylvatica L.): evidence from long-term experimental plots. Eur. J. For. Res. 124, 193–205.
Pretzsch, H., 2019. The effect of tree crown allometry on community dynamics in mixed-species stands versus monocultures. A review and perspectives for modeling and silvicultural regulation. Forests 10, 810.
Pretzsch, H., 2021a. The social drift of trees. Consequence for growth trend detection, stand dynamics, and silviculture. Eur. J. For. Res. 140, 703–719.
Pretzsch, H., 2021b. Tree growth as affected by stem and crown structure. Trees 35, 947–960.
Pretzsch, H., 2022. The emergent past: Past natural and human disturbances of trees can reduce their present resistance to drought stress. Eur. J. For. Res. 141, 87–104.
Pretzsch, H., Rais, A., 2016. Wood quality in complex forests versus even-aged monocultures: review and perspectives. Wood Sci. Technol. 50, 845–880.

Pretzsch, H., Schütze, G., 2009. Transgressive overyielding in mixed compared with pure stands of Norway spruce and European beech in Central Europe: evidence on stand level and explanation on individual tree level. Eur. J. For. Res. 128, 183–204.
Pretzsch, H., Schütze, G., Uhl, E., 2013. Resistance of European tree species to drought stress in mixed versus pure forests: evidence of stress release by inter-specific facilitation. Plant Biol. 15, 483–495.
Pretzsch, H., Ahmed, S., Jacobs, M., Schmied, G., Hilmers, T., 2022. Linking crown structure with tree ring pattern: methodological considerations and proof of concept. Trees 1–19.
Purahong, W., Kapturska, D., Pecyna, M.J., Schulz, E., Schloter, M., Buscot, F., Hofrichter, M., Krüger, D., 2014. Influence of different forest system management practices on leaf litter decomposition rates, nutrient dynamics and the activity of ligninolytic enzymes: a case study from Central European forests. PLoS One 9, e93700.
Pyörälä, J., Saarinen, N., Kankare, V., Coops, N.C., Liang, X., Wang, Y., Holopainen, M., Hyyppä, J., Vastaranta, M., 2019. Variability of wood properties using airborne and terrestrial laser scanning. Remote Sens. Environ. 235, 111474.
Rais, A., Jacobs, M., van de Kuilen, J.-W.-G., Pretzsch, H., 2021. Crown structure of European beech (Fagus sylvatica): a noncausal proxy for mechanical–physical wood properties. Can. J. For. Res. 51, 834–841.
Rawat, M., Arunachalam, K., Arunachalam, A., 2015. Plant functional traits and carbon accumulation in forest. Climate Change Environ. Sustainab. 3, 1–12.
Ripley, B., Venables, W., Ripley, M.B., 2015. Package 'class'. The Comprehensive R Archive. Network 11.
Roussel, J.-R., Auty, D., Coops, N.C., Tompalski, P., Goodbody, T.R.H., Meador, A.S., Bourdon, J.-F., De Boissieu, F., Achim, A., 2020. lidR: An R package for analysis of Airborne Laser Scanning (ALS) data. Remote Sens. Environ. 251, 112061.
Saarinen, N., Kankare, V., Huuskonen, S., Hynynen, J., Bianchi, S., Yrttimaa, T., Luoma, V., Junttila, S., Holopainen, M., Hyyppä, J., 2022. Effects of stem density on crown architecture of Scots pine trees. Front. Plant Sci. 13.
Schmied, G., Hilmers, T., Uhl, E., Pretzsch, H., 2022. The Past Matters: Previous Management Strategies Modulate Current Growth and Drought Responses of Norway Spruce (Picea abies H. Karst.). Forests 13.
Schneider, R., Calama, R., Martin-Ducup, O., 2020. Understanding tree-to-tree variations in stone pine (Pinus pinea L.) cone production using terrestrial laser scanner. Remote Sens. (Basel) 12, 173.
Schweingruber, F.H., 2012. Tree rings: basics and applications of dendrochronology. Springer Science & Business Media.
Shenkin, A., Bentley, L.P., Oliveras, I., Salinas, N., Adu-Bredu, S., Marimon-Junior, B.H., Marimon, B.S., Peprah, T., Choque, E.L., Trujillo Rodriguez, L., 2020. The influence of ecosystem and phylogeny on tropical tree crown size and shape. Front. Forests Global Change 3, 109.
Shinozaki, K., Yoda, K., Hozumi, K., Kira, T., 1964. A quantitative analysis of plant form-the pipe model theory: II. Further evidence of the theory and its application in forest ecology. Japanese J. Ecol. 14, 133–139.
Sievänen, R., Nikinmaa, E., Nygren, P., Ozier-Lafontaine, H., Perttunen, J., Hakula, H., 2000. Components of functional-structural tree models. Ann. For. Sci. 57, 399–412.
Sillett, S.C., Van Pelt, R., Carroll, A.L., Kramer, R.D., Ambrose, A.R., Trask, D.A., 2015. How do tree structure and old age affect growth potential of California redwoods? Ecol. Monogr. 85, 181–212.
Srinivasan, S., Popescu, S.C., Eriksson, M., Sheridan, R.D., Ku, N.-W., 2015. Terrestrial laser scanning as an effective tool to retrieve tree level height, crown width, and stem diameter. Remote Sens. (Basel) 7, 1877–1896.
Stephenson, N.L., Das, A.J., Condit, R., Russo, S.E., Baker, P.J., Beckman, N.G., Coomes, D.A., Lines, E.R., Morris, W.K., Rüger, N., 2014. Rate of tree carbon accumulation increases continuously with tree size. Nature 507, 90–93.
Sundberg, B., Ericsson, A., Little, C.H.A., Näsholm, T., Gref, R., 1993. The relationship between crown size and ring width in Pinus sylvestris L. stems: dependence on indole-3-acetic acid, carbohydrates and nitrogen in the cambial region. Tree Physiol. 12, 347–362.
Tallieu, C., Badeau, V., Allard, D., Nageleisen, L.-M., Bréda, N., 2020. Year-to-year crown condition poorly contributes to ring width variations of beech trees in French ICP level I network. For. Ecol. Manage. 465, 118071.
West, G.B., Enquist, B.J., Brown, J.H., 2009. A general quantitative theory of forest structure and dynamics. Proc. Natl. Acad. Sci. 106, 7040–7045.
Wright, S.J., Bunker, D., Dalling, J., Davies, S., Díaz, S., Engelbrecht, B., Harms, K., Kitajima, K., Kraft, N., Marks, C., 2006. Towards a functional trait based research program within the Center for Tropical Forest Science. The Center for Tropical Forest Science.
Xue, L., Feng, H.-F., Chen, F.-X., 2010. Time-trajectory of mean component weight and density in self-thinning Pinus densiflora stands. Eur. J. For. Res. 129, 1027–1035.
Yen, T.-M., 2015. Relationships of Chamaecyparis formosensis crown shape and parameters with thinning intensity and age. Ann. For. Res. 58, 323–332.